
Chapter 8

Central Pattern Generators

SHARON CROOK and AVIS COHEN

8.1 Introduction

Many organisms exhibit repetitive or oscillatory patterns of muscle activity that produce rhythmic movements such as locomotion, breathing, chewing and scratching. Examples include the escape swimming of the mollusc *Tritonia diomedea*, the digestive rhythms of the lobster, the undulatory swimming movements of the fish or the lamprey, the stepping movements of the cockroach, the rapid wing motion of the locust during flight, and the more complicated locomotion of a quadruped mammal such as the domestic cat. The neuronal circuits that give rise to the patterns of muscle contractions which produce these movements are referred to as *central pattern generators*, or CPGs. Various experimental preparations in which the CPG is isolated from external influence demonstrate that these circuits require no external control for the generation of temporal sequences of rhythmic activity. However, these animals move through the world in an adaptive manner where the same motoneurons are involved in the production of a variety of rhythmic behaviors. Thus, many CPGs are capable of producing multiple patterns of activity in the intact behaving animal (Getting 1989). The ability to switch between different motor behaviors and blend different rhythms relies on feedback from proprioceptors and influence from higher centers of the nervous system; therefore, it is most appropriate to view every CPG as one piece of a distributed control system (Cohen 1992).

One would like to understand how the neurons in a CPG interact and influence one another, how the underlying circuitry of the network produces the collective behavior of the cells, what mechanisms might allow the network to switch among various patterns of

activity, and whether the oscillatory patterns are due primarily to the activity of individual intrinsically oscillatory neurons or to oscillations that are a product of the entire network. The number of cells composing a network that functions as a CPG often determines the manner in which the CPG is studied and the choice of a modeling strategy. Some CPG circuits are anatomically localized and contain a small number of neurons. This occurs most often in CPGs that produce rhythmic behaviors in invertebrates. In these small networks, neurons can be individually identified from animal to animal, permitting detailed circuit descriptions that include cellular and synaptic properties. In contrast to these invertebrate CPGs, there are possibly millions of neurons involved in the production of rhythmic patterns of motor activity in most vertebrates (Murray 1989). In this case, modelers often categorize the neurons into classes that share similar properties so that large networks can be simulated by relatively few cell types (Getting 1989).

The small localized CPGs that occur in invertebrate preparations make it possible to study the relationship between the emergent collective behavior of the biological network and the network's underlying circuitry (Getting 1989). The dynamical properties of many invertebrate CPGs have been analyzed using such techniques as experimental manipulations of cellular, synaptic, and connectivity properties, detailed simulations of the cell interactions within the network, and analytical studies of equations that might describe the network dynamics. For example, Getting created a network simulation of the escape swimming rhythm of the mollusc *Tritonia diomedea* (Getting 1989). This simulation relies on a compartmental model of the network cells with appropriate passive membrane properties, repetitive firing characteristics, and synaptic actions. In addition, the input to the model corresponds to the normal sensory activation of the actual CPG. Some of the properties of Getting's model are demonstrated in the GENESIS simulation *Tritonia*. Another example of an invertebrate CPG that has been studied and modeled extensively is the lobster stomatogastric ganglion. This region contains the neurons that are involved in the generation of the slow rhythm that fires the muscle contractions of the lobster gastric mill and also those that generate the rhythm that controls the muscles of the pyloric region of the lobster stomach (Shepherd 1994). Experimentation with this system has shown that even when a detailed study of the network circuitry provides a qualitative description accounting for the presence of a given motor pattern, there is often no precise explanation for the mechanisms that control the frequency, duration, and phase relations of the motor pattern (Marder and Meyrand 1989). Studies of the invertebrate CPGs mentioned above show that the generation of these rhythms is a complicated process involving the influence of multiple neurotransmitters and modulators that modify the output of the circuit (Marder and Meyrand 1989).

Due to the large number of neurons present in most vertebrate CPG circuits, models of CPGs in vertebrates often involve simplified mathematical representations where a single oscillator may represent many neurons. For example, most models of mammalian locomotion attempt to create an oscillatory network that can account for the production of the alternating flexor-extensor activity responsible for limb coordination during locomotion.

tion (Grillner 1981). In such models, the step cycle of each single limb is represented by the cyclic behavior of an oscillator intended to abstractly represent the collective output of the neurons controlling that limb. Examples of such models include Szekely's model for the locomotion of the salamander (Szekely 1968), and the models of Lundberg and Phillips (1973) and Grillner (1981) for cat locomotion. The lamprey and various types of fish have also been used extensively in studies of vertebrate CPGs. These organisms propel themselves through water by a sequence of rhythmic body undulations caused by traveling waves of contractions that progress down the axial muscles from head to tail. Their swimming patterns have led to models of locomotion consisting of chains of coupled oscillators that represent the state of the oscillatory cells that occur in segments along the spinal cord and control the sequence of muscle contractions along the body during locomotion (Rand, Cohen and Holmes 1988, Cohen and Kiemel 1993, Kopell and Ermentrout 1986). For an overview of such models, see Murray (1989) or Cohen, Ermentrout, Kiemel, Kopell, Sigvardt and Williams (1992).

We must understand the mathematical basis for a model if we hope to use it to gain insight into the behavior of the biological system that it represents. In this chapter, we examine some of the fundamental ideas used in the formulation of models of central pattern generators. These mathematical concepts are reinforced with examples in the form of simulations that can be run using the GENESIS script *CPG*. This script creates a simulation environment consisting of a network of four neurons where the user may interactively change the cell parameters as well as the connections between cells and the synaptic properties of those connections. Before continuing with this chapter, the reader should become familiar with the *CPG* tutorial. Begin by entering the *CPG* simulation environment using the process for running a GENESIS simulation which is described earlier in this book in Sec. 3.3. After entering the simulation environment, click on the **HELP** button located in the control panel at the top center of the screen. The help menu that appears provides some initial instructions under the headings **USING HELP**, **RUNNING THE SIMULATION**, and **MODEL PARAMETERS**. These help texts provide the procedures for experimentally changing the cell parameters, changing the connections between cells, and manipulating the simulation windows. Suggestions of simulation parameters that provide illustrative behaviors for various models are given throughout the remaining sections of this chapter. In the event that the mathematical description of the behavior of a particular model seems unclear, it may be useful to run the simulations before attempting a more detailed study of the mathematical treatment.

8.2 Two-Neuron Oscillators

In this section, we consider models that mimic the behavior of a system of two coupled oscillators in an attempt to understand some of the ways in which biological oscillators may influence one another. Each oscillator can represent a single neuron or a network of cells that collectively function as an oscillator. We first present phase equation models that do not depend on the oscillator structure so that the model results apply to both single cell and network oscillators. We show that these models are simple enough to be analyzed mathematically yet complex enough to capture some of the underlying principles that govern the behavior of a two-oscillator network. Next, we briefly mention a modeling option that uses higher-order systems of equations and incorporates more information about the oscillator structure.

8.2.1 Phase Equation Model of Coupled Oscillators

First consider a general mathematical model due to Rand, Cohen, and Holmes (1988) for a network of two oscillators where each is treated as a simple biological oscillator, ignoring the structure of the oscillation and the mechanisms that produce it. In actuality, the behavior of each oscillatory neuron or network oscillator is determined by a multitude of parameters that can be used to represent the state of the oscillator at any given time. Due to the cyclic behavior of each oscillator, if we draw an orbit in the parameter space that shows how the parameters change with time, the oscillator eventually returns to the same state. This type of orbit is known as a limit cycle. In addition, for small perturbations away from the orbit in the parameter space, the orbit of the oscillator returns to this cycle; that is, the orbit is locally asymptotically stable as shown in Fig. 8.1. These assumptions allow us to test assertions regarding the coordinating system while knowing little about the individual oscillators.

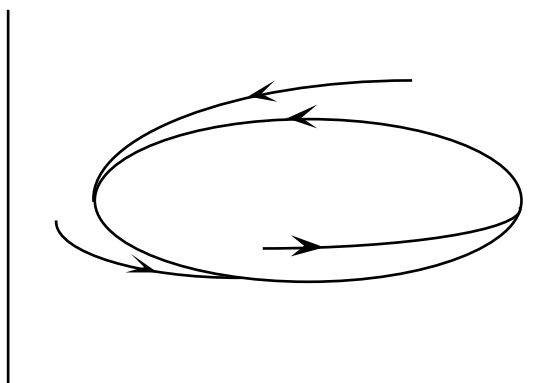


Figure 8.1 Locally asymptotically stable limit cycle in two-dimensional space.

Since we assume that each of the two oscillators in this model can be represented by a structurally stable dynamical system that exhibits a locally asymptotically stable limit cycle, the behavior of each can be represented by a single variable, $\theta_i(t)$ for $i \in \{1, 2\}$, which specifies the position of the oscillator around its limit cycle at time t ; that is, $\theta_i(t)$ specifies the phase of the limit cycle. In addition, we rescale $\theta_i(t)$ so that it flows uniformly around the limit cycle taking values from 0 to 2π radians over one cycle. Thus, $\theta_i(t)$ is proportional to the fraction of the period that has elapsed and the behavior of each oscillator is characterized by the differential equation

$$\dot{\theta}_i(t) = \omega_i, \quad (8.1)$$

where ω_i is the constant frequency of the oscillator, and $2\pi/\omega_i$ is the period. We use modular arithmetic so that $\theta_i(t)$ always lies between 0 and 2π , and the solution to Eq. 8.1 is

$$\theta_i(t) = (\omega_i t + \theta_i(0)) \pmod{2\pi}, \quad (8.2)$$

where $\theta_i(0)$ is the initial value of θ_i . When two such oscillators are coupled, we obtain a system of equations

$$\dot{\theta}_1(t) = \omega_1 + h_{12}(\theta_1, \theta_2) \quad (8.3)$$

$$\dot{\theta}_2(t) = \omega_2 + h_{21}(\theta_2, \theta_1), \quad (8.4)$$

where $h_{ij}(\theta_i, \theta_j)$ represents the coupling effect of the j th oscillator on the i th oscillator. This coupling term must be 2π periodic since we would like the rate of change to depend only on the oscillator phase and not on the number of cycles that have already occurred or the amplitude of the oscillation. Since the behavior of each cell is described using only the phase, the coupling also depends only upon the phase.

It is often convenient to define a quantity

$$\phi(t) = \theta_1(t) - \theta_2(t) \quad (8.5)$$

which represents the difference between the phases or the phase lag of oscillator 2 relative to oscillator 1. Note that like θ_i , $\phi(t) \in [0, 2\pi)$. Combining Eqs. 8.3 and 8.4, we obtain

$$\dot{\phi}(t) = \dot{\theta}_1(t) - \dot{\theta}_2(t) \quad (8.6)$$

$$= (\omega_1 - \omega_2) + (h_{12}(\theta_1, \theta_2) - h_{21}(\theta_2, \theta_1)). \quad (8.7)$$

Much of the analytical work to date on coupled oscillators deals with interactions that depend only on the difference between the phases. Consider the simplest case where h_{ij} depends only on the phase lag, and in addition $h_{ij}(\theta_i, \theta_j) = 0$ when the phase lag between the i th and j th oscillators is zero. This is known as *diffusive coupling*. For example, if we let $h_{ij} = a_{ij} \sin(\theta_j - \theta_i)$, we obtain

$$\dot{\phi}(t) = (\omega_1 - \omega_2) - (a_{12} + a_{21}) \sin(\phi(t)). \quad (8.8)$$

This equation can be solved exactly, but let us consider those solutions where 1 : 1 phase-locked motion occurs; that is, consider the situation where the phase lag between the two oscillators remains constant. This type of motion occurs when $\dot{\phi}(t) = 0$. Equating the right-hand side of Eq. 8.8 to zero, we obtain

$$\phi = \arcsin\left(\frac{\omega_1 - \omega_2}{a_{12} + a_{21}}\right) \quad (8.9)$$

which has zero, one, or two solutions depending on the value of the ratio of the frequency difference $\omega_1 - \omega_2$ to the net coupling strength $a_{12} + a_{21}$. When the net coupling is small enough, the ratio has absolute value greater than unity. Since the sin function takes values only between -1 and 1 , there is no solution to Eq. 8.9 in this case, and the oscillators will drift with respect to one another. As the coupling is increased, a critical value is reached where the frequency difference is equal to the net coupling strength. At this point, the absolute value of the ratio is 1 , and the system goes into phase-locked motion. If the net coupling is positive or excitatory, then the faster oscillator leads the phase-locked motion by a phase of between 0 and 90 degrees. If the net coupling is negative or inhibitory, the slower oscillator leads by between 90 and 180 degrees.

8.2.2 Simulation Parameters

To interactively study some of the phenomena exhibited by this model, create a simulation of two coupled biological oscillators using the *CPG* tutorial. Begin by changing the strengths of all of the connections to zero so that the simulation environment consists of four isolated cells. We would like the cells labeled “L1” and “R1” to function as two biological oscillators that can be simulated by supplying a constant current injection to the somata of these two cells. Bring up the windows that allow the user to interactively change the inputs to these two cells by clicking on the appropriate toggles under the heading `inputs`. Set the injection current to the soma of L1 to $0.00025 \mu A$ with zero delay and a duration that is greater than the number of steps for the simulation such as 200 msec . The result is a constant current injection throughout the duration of the simulation which causes the continuous firing of the cell. Likewise, create an injection current of $0.0003 \mu A$ to the soma of R1 in the same manner. Make sure that all other possible inputs, including those to L2 and R2, are set to zero current. Don’t forget to hit the “Return” key after any change is made within a dialog box and to click on the `APPLY` button after all of the changes have been made for a single desired input current. After the above changes have been made, click on the `STEP` button to run the simulation. It is important to remember that we are assuming that these two cells are intrinsically oscillatory so that they oscillate continuously, where R1 has a slightly greater intrinsic frequency due to the larger injection current.

Now add coupling between the two cells, starting with small mutually excitatory coupling. This can be done by setting the coupling strength of the connection from L1 onto

R1 to 5 and making sure that the toggle for that connection is in the excitatory mode. Set the strength of the connection from R1 onto L1 to 5 in a similar manner. After running the simulation, the graphs reveal that the two oscillating cells are drifting with respect to one another. In other words, the coupling is too weak to cause phase-locked behavior. Now gradually increase the coupling strength between the two cells by increments of 5, clicking on the `RESET` and `STEP` buttons after each change in order to observe the behavior of the system. As the coupling strength is increased, eventually the system exhibits behavior that converges to phase-locked oscillations where the cell with the greater intrinsic frequency, namely, R1, leads. This causes the frequency of oscillation of the system to be greater than the intrinsic frequency of L1. Now repeat the process outlined above for inhibitory connections, beginning with weak mutually inhibitory coupling and gradually increasing the coupling strength. In this case, stronger coupling strengths are required for phase-locked behavior due to the nature of the inhibitory connections in the simulation environment as explained in the text of the help selection under `MODEL PARAMETERS`. During the phase-locked oscillations, the cell with the slower intrinsic oscillation will lead, causing the frequency of the system to be smaller than the intrinsic frequency of R1.

8.2.3 Initial Conditions

In the qualitative analysis of any system of differential equations, it is important to consider the role of the initial conditions since the system behavior depends on these initial values. Consider a *CPG* simulation architecture that demonstrates the crucial role of the initial conditions for the two-oscillator model presented in Sec. 8.2.1. Begin by changing the current injections to L1 and R1 so that they are identical, say, $0.00015 \mu A$. In this case the two oscillators have identical intrinsic frequencies; that is, $\omega_1 = \omega_2$. Since the frequency difference $\omega_1 - \omega_2$ is zero, Eq. 8.9 indicates that there are two solutions that provide phase-locked behavior, $\phi = 0$ and $\phi = \pi$. Thus, the two oscillators may be phase-locked with no phase lag so that they demonstrate synchronous behavior, or they may be phase-locked 180 degrees out of phase. We can obtain these two types of behavior by varying the initial conditions of the system.

First, set the delays for both cells to zero and make sure that the durations are set to 200 *msec*. Begin with symmetric mutually excitatory coupling with the coupling strength of each connection set to 20. Run the simulation and observe that the two cells begin firing in phase due to their identical initial values and continue to fire in phase due to the symmetry of the network. Next change the delay of R1 to 15 *msec*. In this case, we are effectively changing the initial conditions of the system so that we begin with two cells that are firing out of phase at time $t = 15 \text{ msec}$. As predicted for the case where the intrinsic frequencies of the two oscillators are identical, the cells still exhibit phase-locked motion; however, they fire out of phase. This demonstrates how important initial conditions may be for the production of different temporal patterns of activity in these simplified models. However,

the initial conditions do not play such a crucial role in biological system where noise and inherent differences prevent any two oscillators from having identical frequencies.

8.2.4 Synaptic Coupling

Naturally, the phase equation model described above is not sufficient for predicting or studying all possible types of behavior exhibited by two coupled neurons or network oscillators. In particular, the choice of diffusive coupling may be limiting. Although diffusive coupling probably models the behavior of electrical coupling between multiple cells accurately, in general we would not expect the synaptic interactions between two neurons to depend exclusively on the difference between the phases. For example, with diffusive coupling a phase difference of zero results in a coupling term with a value of zero so that two neurons that are exhibiting identical behavior have no influence on one another. Because this does not seem biologically plausible for synaptic connections between neurons, Ermentrout and Kopell (1990) consider a model that differs slightly from the previous one and contains coupling terms that behave more like synaptic coupling between cells. The assumptions for this coupling hold true for Hodgkin-Huxley-like neural models in which the coupling is due to voltage only (Ermentrout and Kopell 1990). In the following description of the model, we assume that the oscillators are identical for ease of analysis.

The equations for this model are

$$\dot{\theta}_1 = \omega_1 + p(\theta_2)r(\theta_1) \quad (8.10)$$

$$\dot{\theta}_2 = \omega_2 + p(\theta_1)r(\theta_2), \quad (8.11)$$

which are simply Eqs. 8.3 and 8.4 with $h_{ij}(\theta_i, \theta_j) = p(\theta_j)r(\theta_i)$, where p is a periodic smooth pulse function and r plays a role that is analogous to that of a *phase response curve*. A phase response curve, or PRC, for a given oscillator and a given brief stimulus is determined experimentally by stimulating the oscillator and waiting until the system relaxes back to its oscillation with a shift in phase. The PRC can be represented by a function $\hat{r}(\theta)$ that gives the phase shift and depends upon the phase θ at which the stimulus is administered. Consider the situation where the relaxation time is short relative to the time between stimuli τ . Let θ^k be the phase just before the k th stimulus so that we obtain a sequence of phases $\{\theta^k\}$ that are related by the difference equation

$$\theta^{k+1} = \omega\tau + \theta^k + \hat{r}(\theta^k), \quad (8.12)$$

where ω is the natural frequency of the oscillator. We can rewrite Eq. 8.12 as the differential equation

$$\dot{\theta} = \omega + \delta(t \bmod \tau)\hat{r}(\theta), \quad (8.13)$$

where δ is the Dirac delta function that provides a pulse stimulus at intervals a time τ apart. According to Ermentrout, since real stimuli are not instantaneous, it is reasonable

to replace δ with the smooth distributed stimulus function p . In doing so, we obtain an equation analogous to Eqs. 8.10 and 8.11, where r represents the phase response curve \hat{r} . That is, the coupling mimics the effects of coupling two oscillators via their PRC's.

Ermentrout and Kopell show that for this type of coupling, the phase equation model exhibits qualitative behavior that is similar to that of more complex non-phase equation models such as those discussed briefly in the following section. In particular, as the coupling strength increases, the system may go from phase drift to phase-locking and finally to a phenomenon known as *oscillator death*. Oscillator death corresponds to a critical point solution for the system since the oscillator remains at a constant state in the parameter space. In addition, the critical point must be asymptotically stable in order for the oscillator death to be robust. Otherwise, small perturbations would result in a return to oscillatory behavior. This type of behavior cannot occur in the model defined by Eqs. 8.3 and 8.4 since no asymptotically stable critical point exists for that system. However, Ermentrout and Kopell prove that for synaptic coupling, oscillator death is a robust phenomenon for sufficiently large interactions. In addition, they show that the replacement of the stable limit cycle by a stable critical point can also occur in chains of oscillators with coupling between nearest neighbors like those discussed in Sec. 8.3.1. This fact is of interest for the study of models of locomotion that are composed of chains of coupled oscillators such as the Rand, Cohen and Holmes (1988) model for lamprey locomotion mentioned earlier.

8.2.5 Non-phase Equation Models

The greatest strength of the two models discussed above is their relative simplicity. Phase equation models that allow a single equation to represent the dynamics of an individual cell make it possible to conduct a qualitative analysis of the dynamics of the system. This type of mathematical analysis is much more difficult in higher-order systems of equations. For example, consider the Hodgkin-Huxley model for the biophysics of the squid giant axon, described in Chapter 4. In this model, a system of four differential equations (Eq. 4.1 and Eqs. 4.11–4.13) is used to characterize the ion concentration changes that result in the production of an action potential in a single oscillatory neuron. Thus, a system of eight equations with the appropriate coupling terms is required to capture the behavior of two coupled neurons. Unlike the reparameterized phase equation model, this system of eight equations contains useful information about the manner in which specific parameters change during the oscillatory activity. However, due to the large number of equations required, more detailed models are difficult to study analytically, and simulations must be used to numerically reproduce behavior. Such simulations allow the user to interactively observe the output of the model in an attempt to understand the interactions of the neurons within the system by studying the relationships among the model parameters. The *CPG* simulation environment for GENESIS that is discussed throughout this chapter is an implementation of the Hodgkin-Huxley equation model. For this reason, the range of behavior demonstrated by

the simulation is more complex than the behavior of the phase equation model of coupled oscillators discussed above; however, some basic interactions can be understood in the context of the phase equation model.

8.3 Four-Neuron Oscillators

Now that we have discussed some of the basic principles that govern the behavior of two coupled oscillators, we would like to apply these ideas to slightly larger networks. As previously mentioned, larger networks are more difficult to analyze mathematically since they require more equations, and thus we will eventually rely on simulations in our attempt to understand their behavior. In this section we examine chains of four oscillators with nearest-neighbor coupling as well as more complex architectures with various types of coupling among four oscillatory cells. We attempt to explore some of the basic ideas used to formulate the vertebrate CPG models mentioned in Sec. 8.1. In particular, the discussion of chains of four coupled oscillators that follows provides insight into various models for lamprey locomotion and the locomotion of some types of fish. These models are inspired by the fact that the waves of muscle contractions that produce locomotion in these organisms are induced by periodic bursts of activity in the ventral roots that emerge at each segment of the spinal cord. The phase lag in activity between segments is proportional to the distance between the points, indicating a constant speed traveling wave of contractions (Rand et al. 1988, Kopell and Ermentrout 1986). Following the discussion of chains of coupled oscillators, we construct networks capable of producing patterns of activity that mimic various gaits for tetrapod locomotion. In these gait simulations, the phase relations among the various oscillators in the CPG model are important since they represent the phase relations among the limbs during locomotion.

8.3.1 Chains of Coupled Oscillators

We begin by extending the concepts outlined in Sec. 8.2.1 in order to develop a phase equation model for a chain of four coupled oscillators. The following treatment appears in Rand et al. (1988) in a more general form for chains of n oscillators. We would like the chain to have only nearest-neighbor coupling with no long-range connections. Thus, Eqs. 8.3 and 8.4 are extended to a system of four differential equations of the form

$$\dot{\theta}_1(t) = \omega_1 + h_{12}(\theta_1, \theta_2) \quad (8.14)$$

$$\dot{\theta}_2(t) = \omega_2 + h_{21}(\theta_2, \theta_1) + h_{23}(\theta_2, \theta_3) \quad (8.15)$$

$$\dot{\theta}_3(t) = \omega_3 + h_{32}(\theta_3, \theta_2) + h_{34}(\theta_3, \theta_4) \quad (8.16)$$

$$\dot{\theta}_4(t) = \omega_4 + h_{43}(\theta_4, \theta_3). \quad (8.17)$$

As before, we assume diffusive coupling and let $h_{ij} = a_{ij} \sin(\theta_j - \theta_i)$. However, we use a uniform coupling strength $a_{ij} = a$ for ease of analysis. Again, we define the quantity

$$\phi_i(t) = \theta_i(t) - \theta_{i+1}(t) \quad (8.18)$$

to represent the phase lag between oscillators for $i \in \{1, 2, 3\}$. So, our system of equations can be represented by the vector equation

$$\dot{\phi}(t) = \Omega + AS(t), \quad (8.19)$$

where

$$\phi(t) = \begin{bmatrix} \phi_1(t) \\ \phi_2(t) \\ \phi_3(t) \end{bmatrix}, \quad (8.20)$$

$$\Omega = \begin{bmatrix} \omega_1 - \omega_2 \\ \omega_2 - \omega_3 \\ \omega_3 - \omega_4 \end{bmatrix}, \quad (8.21)$$

$$A = a \begin{bmatrix} -2 & 1 & 0 \\ 1 & -2 & 1 \\ 0 & 1 & -2 \end{bmatrix}, \quad (8.22)$$

and

$$S = \begin{bmatrix} \sin(\phi_1(t)) \\ \sin(\phi_2(t)) \\ \sin(\phi_3(t)) \end{bmatrix}. \quad (8.23)$$

As in the previous sections, we are interested in 1 : 1 phase locked motion where the phase lags remain constant; therefore, we would like to find solutions to the equation $\dot{\phi} = 0$. Note that $\dot{\phi} = 0$ when $S = -A^{-1}\Omega$, and we know that

$$A^{-1} = \frac{-1}{4a} \begin{bmatrix} 3 & 2 & 1 \\ 2 & 4 & 2 \\ 1 & 2 & 3 \end{bmatrix}. \quad (8.24)$$

If we assume that there is a smooth gradient in the intrinsic frequency of oscillation along the cord, then the frequency difference along the chain is constant, and $\omega_1 - \omega_2 = \omega_2 - \omega_3 = \omega_3 - \omega_4 = c$. In this case,

$$\Omega = c \begin{bmatrix} 1 \\ 1 \\ 1 \end{bmatrix} \quad (8.25)$$

and substituting, we obtain

$$S = \frac{c}{2a} \begin{bmatrix} 3 \\ 4 \\ 3 \end{bmatrix}. \quad (8.26)$$

Since the entries of the vector S are sin functions,

$$\left| \frac{c}{a} \right| \leq \frac{1}{2} \quad (8.27)$$

is a necessary and sufficient condition for the existence of 1 : 1 phase-locked motion. When this condition holds, the resulting motion is frequency-locked at the average frequency of the uncoupled oscillators (Rand et al. 1988). The oscillations create a traveling wave of activation along the chain unless the oscillators all have identical intrinsic frequencies. When the frequencies are identical, there is no phase difference along the chain, $c = 0$, and the oscillators behave synchronously with the exception of those at each end of the chain. The oscillators at the two ends of the chain are subject to the influence of only one neighboring cell, and thus behave slightly differently than the internal cells of the chain that are influenced by two neighbors. Kopell and Ermentrout extend this model by replacing the diffusive coupling with the synaptic coupling described in Sec. 8.2.4. Their model generates a constant speed traveling wave of contractions without the presence of a gradient of oscillator frequencies along the cord (Kopell and Ermentrout 1986).

8.3.2 Simulation Parameters

To observe the behavior described in the section above which is similar in principle to the behavior of a swimming fish (albeit with few segments), create a simulation of a chain of biological oscillators with nearest-neighbor coupling using the *CPG* tutorial. First, set all of the connection strengths to zero so that the simulation environment consists of four isolated cells. To simulate the behavior of oscillatory cells with identical intrinsic frequencies, set the injection current to the soma of each cell to $0.0002 \mu A$ with zero delay and a duration that is greater than the number of steps for the simulation. Set all other inputs to zero, and be sure to click on **APPLY** after all of the changes have been made for a desired injection current. Click on the **STEP** button to run the simulation, and check to be sure that all four cells are oscillating in an identical manner.

Now build the connections required for a chain of four oscillators with nearest-neighbor coupling as shown in Fig. 8.2. Make sure that the connections are excitatory with identical connection strengths. The choice of connection strength is not important at this point; a connection strength of around 20 will suffice. When you click on **STEP** to run the simulation, you should discover that the oscillators in the chain oscillate in synchrony with the exception of the oscillators on the end of the chain which behave differently due to the

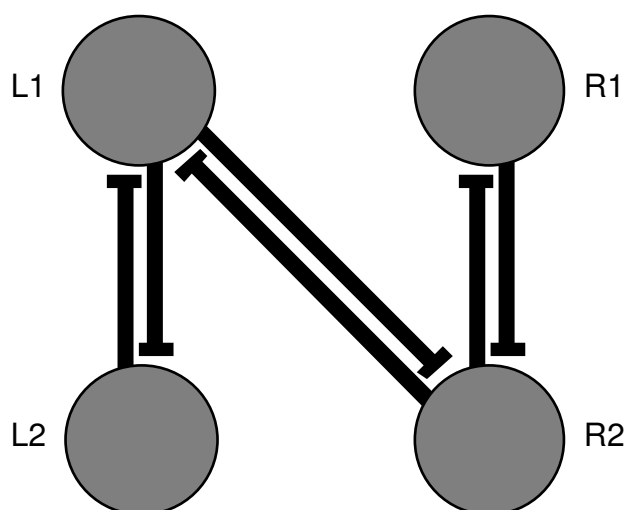


Figure 8.2 Simulation architecture for a chain of four oscillators with nearest-neighbor coupling. All connections are excitatory with identical strengths.

end conditions. This is the behavior predicted by the model in the case when there is no difference in oscillator frequencies along the chain so that $c = 0$.

Next change the injection currents to the cells causing the cells to have varying intrinsic frequencies with a constant difference in frequency along the chain. For example, you might use values of 0.00035, 0.0003, 0.00025, and 0.0002 μA as the injection inputs along the chain. In this case, the model predicts a traveling wave of activation provided that the value of the connection strength is large enough. Begin with very small values for the identical connection strengths and gradually increase the value until you see a wave of activation. It may be difficult to see the wave since each one begins before the previous wave has reached the end of the chain.

It is also possible to obtain a wave of activation in a chain of neurons simply by causing the first cell in the chain to fire. Each cell activates the next so that the activation moves down the length of the chain. To simulate this type of activity, set the injection input to the soma of the first cell in the chain to 0.0002 μA for a duration of several milliseconds, and set all other possible inputs to zero. This will cause a single wave of activation; however, this model requires outside control for continuous behavior since multiple waves require repeated inputs to the first oscillator at the desired temporal intervals. For this reason, the behavior is less robust than that of the model described above which uses intrinsic oscillators to create continuous waves of behavior in the absence of any external influence to the CPG.

8.3.3 Modeling Gaits

During tetrapod locomotion, interlimb coordination causes different combinations of limbs to be on or off the ground at the same time as the gait of an animal varies. Each limb moves through a step cycle that consists of a swing phase and a stance phase. During the swing phase, the limb is lifted and brought forward, mostly due to the effort of the flexor muscles. During the stance phase, extensor activity is dominant and provides force to thrust the animal forward (Grillner 1981). The most common mode of coordination among limbs is strict alternation between the two limbs of the same girdle; that is, the movements of the two hindlimbs alternate with each other, and the movements of the two forelimbs alternate with each other. These are known as the alternating gaits which include the walk, pace and trot and are seen in a variety of organisms from the millipede to humans. The differences among these three gaits depend on the timing between the forelimbs and hindlimbs. We refer to all other gaits as non-alternating gaits which include the gallop, canter, half bound, and leaping gaits. Most animals prefer to use different gaits at different velocities, but the gait is not directly linked to the speed (Grillner 1981).

We want to model the patterns of limb coordination required for some of the various gaits mentioned above. In these simulations we let one intrinsic oscillator represent the population of cells that controls the cyclic flexor-extensor activity of a single limb. To begin, click on the **DEFAULTS** button in the main control panel to return to the default architecture provided with the *CPG* simulation. In this default network architecture, the cell labeled L1 represents the left forelimb, R1 represents the right forelimb, L2 represents the left hindlimb, and R2 represents the right hindlimb. Note that all connection strengths are set to a value of 100. Hit **STEP** and observe the pattern of activation that emerges from the network circuitry. As shown in Fig. 8.3, this pattern of activity is the sequence observed in a walking gait. The lateral symmetric inhibitory connections between the two forelimbs and between the two hindlimbs encourage the alternating phase-locked behavior required for all alternating gaits. The excitatory connections help maintain a robust pattern of activation where each oscillator stimulates the next one in the sequence. The remaining inhibitory connections discourage the oscillators from becoming active out of turn. Also, note that the delays are set to values that initialize the simulation with the sequence of activation required for a walking gait. Experimenting with the delays reveals that a variety of initial conditions will lead to this same pattern of behavior although the amount of time required for convergence to phase-locked oscillations varies for different initial conditions. It is important to make sure that the delays are not all identical since beginning the oscillators in phase results in completely synchronous firing due to the symmetry of the network.

Now, alter the architecture so that the vertical connections between L1 and L2 and between R1 and R2 are inhibitory, and make all of the cross-connections excitatory. In addition, change the delays so that L1 and R2 have delays of zero, and L2 and R1 have delays of 15. Click on **RESET** and then run the simulation. This pattern of activity mimics

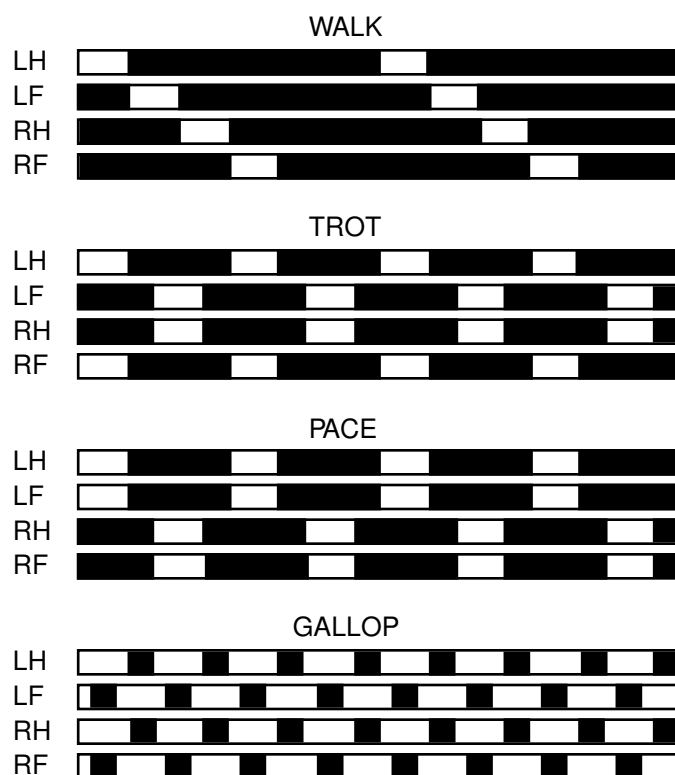


Figure 8.3 Idealized diagram of the stepping movements of the cat for different characteristic gaits. Open bars represent a lifted foot, and closed bars denote a planted foot. Figure adapted from Pearson (1976).

that required for a trotting gait. A similar architecture, where the roles of the left and right forelimbs are switched, provides the pattern of activity required for a pace. In some of the exercises that follow we outline changes in oscillator frequency, initial conditions, and coupling which provide additional gaits and demonstrate some of the ways that these factors can influence the network activity.

In each case, there are many other architectures that will exhibit the same patterns of activity as those mentioned for the various gaits described above and in the exercises. At present, there is little known regarding the mechanisms employed by CPGs in behaving animals. Thus, it is impossible to determine which architectures most closely model these biological mechanisms. Experiments that study CPG-produced locomotion in the cat use treadmill speed to demonstrate that sensory input can lead to gait changes. The stimulation of the mesencephalic locomotor region in these experiments shows that descending drive from higher centers of the nervous system can lead to gait changes as well. Therefore, it seems likely that biological systems may use various methods or combinations of methods

for changing gaits.

8.4 Summary

We are not suggesting that the models and simulations described in this chapter accurately describe how CPGs produce observed patterns of behavior. It is certain that the actual mechanisms are much more complicated and that feedback from proprioceptors and influence from higher centers of the nervous system play an enormous role in the selection and maintenance of robust patterns of activity. However, we believe that this discussion demonstrates how mathematical models and simulations can help us learn to ask the correct types of questions when probing biological systems, and perhaps provide insight into the complex interactions involved in the production of repetitive motor activity.

8.5 Exercises

1. Consider a simulation architecture in which L1 and R1 are identical where each has an input of $0.00015 \mu A$, a delay of zero, and a duration of 200 msec . Implement symmetric mutually excitatory coupling with connection strengths of 1500, and gradually increase the strengths by increments of 100. How might one explain the observed behavior? What happens when the symmetry is broken; that is, what happens when the coupling strengths are unequal, the injection currents are unequal, or the initial conditions differ?
2. It is interesting to note that a fish is capable of swimming backwards when placed in a corner (Grillner 1974). Consider the architecture and parameters for a chain of oscillators described in Sec. 8.3.2. Try experimenting with the parameters to cause the wave to travel in the opposite direction and consider the implications for possible mechanisms for reversing the direction of the wave propagation in a fish.
3. Figure 8.3 shows that the pattern of activity for the idealized gallop is identical to that for the walking gait except that the speed is more rapid. Alter the default architecture provided for the walking gait to create a faster gait that is comparable to a gallop. Begin by simulating an increase in the frequency of the intrinsic oscillations via an increase in the current injection.
4. In a true gallop, there is a lag between the planting of the left forelimb and the right forelimb. Alter the architecture for the idealized gallop that was developed in the preceding question to obtain this asymmetry. Begin by introducing asymmetries in the connection strengths.

-
5. In Sec. 8.3.3 we mention that the differences between the various alternating gaits depend on the timing between the forelimbs and hindlimbs. In fact, the transition from walking to trotting is continuous. As the locomotion speed increases, each forelimb begins to step before the opposite hindlimb touches the ground until the opposite legs step at the same time resulting in a trotting gait (Pearson 1976). Try to mimic the transition from a walk to a trot by making incremental alterations to the architecture and initial conditions.
 6. In various experiments, both picrotoxin and strychnine, which block inhibitory synapses, induce changes in the motor output pattern of several different organisms (Rand et al. 1988). These changes involve a transformation from an out-of-phase mode of oscillation to an in-phase mode. Delete the inhibitory synapses in the various gait simulation architectures discussed in this chapter and in the exercises above. In each case, do the effects of the blocked inhibition support the choice of architecture or suggest that an alternate choice might be more biologically plausible?
 7. Use the insight gained from the various models in this chapter and the gait simulation architectures discussed above to create architectures that simulate the non-alternating gaits such as the canter, leap, and half bound.

